859



R and D CENTER
LABORATORY
TECHNICAL REPORT

NO. TR 12692

# FINITE ELEMENT ANALYSIS OF GROUND DEFORMATIONS BENEATH MOVING TRACK LOADS

Final Report on

Contract DAAE07-81-C4028
Amendment P00002

April 1983

by Leslie L. Karafiath
Research & Development Center
Grumman Aerospace Corporation
Bethpage, New York 11714



U.S. ARMY TANK-AUTOMOTIVE COMMAND
RESEARCH AND DEVELOPMENT CENTER
Warren, Michigan 48090

Technical Report No. TR 12692

Grumman R&D Center Report RE-662

# FINITE ELEMENT ANALYSIS OF GROUND DEFORMATION BENEATH MOVING TRACK LOADS

Final Report

by

Leslie L. Karafiath
Research & Development Center
Grumman Aerospace Corporation
Bethpage, New York 11714

Prepared Under Contract DAAE07-81-C4028
Amendment P00002

for

U.S. Army Tank-Automotive Command
Research and Development Center
Warren, Michigan 48090

April 1983

Approved by: Richard A. Scheuing
Director of Research

Approved for public release;
Distribution Unlimited

UNCLASSIFIED

SECURITY CLASSIFICATION OF THIS PAGE *(When Data Entered)*

| REPORT DOCUMENTATION PAGE | | READ INSTRUCTIONS BEFORE COMPLETING FORM |
|---|---|---|
| 1. REPORT NUMBER<br>TR 12692 | 2. GOVT ACCESSION NO. | 3. RECIPIENT'S CATALOG NUMBER |
| 4. TITLE *(and Subtitle)*<br>Finite Element Analysis of Ground Deformations Beneath Moving Track Loads | | 5. TYPE OF REPORT & PERIOD COVERED<br>6. PERFORMING ORG. REPORT NUMBER |
| 7. AUTHOR*(s)*<br>Leslie L. Karafiath | | 8. CONTRACT OR GRANT NUMBER*(s)*<br>DAAE07-81-C-4028 |
| 9. PERFORMING ORGANIZATION NAME AND ADDRESS<br>Grumman Aerospace Corporation<br>Research and Development Center<br>Bethpage, New York 11714 | | 10. PROGRAM ELEMENT, PROJECT, TASK AREA & WORK UNIT NUMBERS |
| 11. CONTROLLING OFFICE NAME AND ADDRESS<br>U.S. Army Tank-Automotive Command<br>Research and Development Center<br>Warren, MI 48090 | | 12. REPORT DATE<br>13. NUMBER OF PAGES |
| 14. MONITORING AGENCY NAME & ADDRESS*(if different from Controlling Office)*<br>U.S. Army Tank-Automotive Command<br>Research and Development Center<br>Warren, MI 48090 | | 15. SECURITY CLASS. *(of this report)*<br>UNCLASSIFIED<br>15a. DECLASSIFICATION/DOWNGRADING SCHEDULE |

16. DISTRIBUTION STATEMENT *(of this Report)*

Approved for public release; Distribution unlimited

17. DISTRIBUTION STATEMENT *(of the abstract entered in Block 20, if different from Report)*

18. SUPPLEMENTARY NOTES

19. KEY WORDS *(Continue on reverse side if necessary and identify by block number)*

Finite element, Ramberg-Osgood, nonlinear stress-strain properties, soil deformation, motion resistance, travel velocity, track, pressure distribution, moving track load

20. ABSTRACT *(Continue on reverse side if necessary and identify by block number)*

A methodology, using finite element analysis techniques, has been developed for the determination of the deformation of clay soils under moving track loads. The Ramberg-Osgood formula has been used to represent the nonlinear stress-strain properties of clay soils. The DYCAST finite element code of nonlinear , elastic-plastic, dynamic structural analysis has been used for the determination of ground deformations beneath moving track loads. The effect of variations in pressure distribution and speed of travel on ground deformation and associated motion resistance has been analyzed and found to be

DD FORM 1 JAN 73 1473 EDITION OF 1 NOV 65 IS OBSOLETE

UNCLASSIFIED

SECURITY CLASSIFICATION OF THIS PAGE *(When Data Entered)*

significant.

## PREFACE/ACKNOWLEDGEMENT

The work reported herein was performed for the Tank-Automotive Concepts Laboratory of the U.S. Army Tank-Automotive Command (TACOM) Research and Development Center, Warren, Michigan, under the general supervision of Mr. Otto Renius, Director of the Laboratory, and Mr. Zoltan J. Janosi, Chief, Applied Research Function. Mr. Janosi was also technical monitor. Their help and valuable suggestions in carrying out this work are gratefully acknowledged.

Acknowledgement is also due to Dr. Allan Pifko, Senior Staff Scientist of the Grumman R&D Center and one of the principal developers of the DYCAST code, and Ms. Patricia Ogilvie, Senior Program Analyst, for incorporating the time delayed loading option in the code, and for their cooperation in resolving problems encountered in running the program.

CONTENTS

# 1. INTRODUCTION

The major portion of the motion resistance forces encountered by vehicles traveling off-road is caused by the deformation of the ground under the vehicle load. Tracks were originally conceived as implements to distribute the vehicle load over a large area and thereby reduce the pressure to, and deformation of the ground. Tracked vehicles with rigid suspension systems distribute ground pressures nearly evenly and can, at low speed, traverse soft terrain not negotiable by other vehicles.

The requirement of the military for increased cross-country mobility of combat and support vehicles lead to the development of flexible tracks supported by sprung road wheels. While such suspension systems and tracks are necessary for good riding quality at high speed and for obstacle crossing capability, the role of the track in uniformly spreading the pressure over the ground contact area has been severely compromised. The pattern of pressure distribution beneath the tracks of military vehicles, as many measurements show, is characterized by peaks immediately beneath the road wheels rather than by uniformity over the contact area.

The soil response to nonuniform pressure distribution depends on the magnitude of the peak stresses and, if these induce plastic flow conditions in the soil, the duration of the peak stress impulses. The latter is inversely proportional to the velocity of travel. Researchers in the field of off-road mobility have long been intrigued by the idea of reducing motion resistances by increasing the speed of travel. This report presents a methodology which supplants intuition with an analytical tool suitable for the quantitative evaluation of the effect of both pressure distribution and travel velocity on motion resistance.

## 2. SCOPE OF WORK

The general scope of work is to develop a methodology suitable for the analysis of the effect of travel velocity and variations in pressure distribution beneath tracks on ground deformations and associated motion resistance forces. The first phase of the work reported herein treats frictionless (clay) soils only. The scope of work of this phase includes the following items:

- Development of a finite element mesh for the representation of soil continuum and its response to moving track loads
- Evaluation of the suitability of the Ramberg-Osgood formula for representing the nonlinear stress-strain properties of clay soils
- Adaptation of the DYCAST code of nonlinear, elastic-plastic, dynamic structural analysis to the problem of determining soil deformation beneath moving track loads
- Analysis of the effect of variations in pressure distribution and speed of travel on ground deformation.

## 3. MODELING OF SOIL PROPERTIES IN VEHICLE-TERRAIN INTERACTION SIMULATION

The interaction between off-road vehicles and terrain is essentially a contact problem where the geometry of the running gear-soil interface as well as the stresses acting on it change with the operating conditions of the vehicle and the properties of the soil traversed. The solution of the problem requires that there be compliance between the interface geometry and stresses computed for the vehicle running gear and soil. Solution procedures to this exceedingly complex problem proposed by various researchers working in the field of off-road mobility, invariably resorted to simplifying idealizations. In regard to the vehicle, the most commonly adopted simplification is the assumption that the vehicle is moving at a steady, low speed. Even so, solutions based on empiricism or analogies have been preferred over analytical solutions by many who considered analytical formulations unsolvable. In these approaches a major consideration in modeling soil behavior has been the convenience of obtaining some description of soil properties in the field rather than modeling soil behavior by material constants used in the applicable theory of soil behavior.

The most widely used soil property models in this category are:

- Cone Index. Theoretical justification for representing soil properties by cone penetration resistance in pneumatic tire-soil interaction was furnished by Freitag. He showed by dimensional analyses that in purely cohesive soils the cone index and in purely frictional soils the gradient of the cone index is the significant parameter which controls tire performance. Under any other conditions, the use of the cone index distorts the similarity and results in a low confidence level of the performance estimates based on its value.
- Parameters of Pressure Sinkage Relationships. These parameters, obtained from plate-sinkage tests, are of variable dimensions and, therefore, conceptually incorrect. Their use for the determination of the vertical stresses at the running gear-soil interface is based on false analogy and is unsupportable by theory.

The advances in computer sciences and the general availability of computers for the numerical solution of nonlinear differential equations have changed the premises of the treating of vehicle-terrain interaction problems radically, and have made a rational approach to the formulation of these problems possible. In a rational approach, the properties of soil are modeled by the material constants which occur in the theory used for evaluating soil behavior in the interaction problem. Soil property models in this category are:

- Coulomb Strength (Cohesion & Friction Angle). Soil strength has long been recognized as the most important soil property governing mobility. Therefore, it is logical to use strength parameters for the characterization of soil behavior. The strength of soil defines the conditions for plastic state of stresses in the soil. Plasticity theory can be used for the determination of critical stress conditions occurring in various vehicle-terrain interaction problems. However, strength parameters by themselves are insufficient for the characterization of soil deformation behavior and, therefore, in vehicle-terrain interaction models based on plasticity theory various semi-empirical relations had to be used for the estimation of soil deformations

- Stress-Strain Properties. Early attempts to model the behavior of soil as a linear elastic material were of extremely limited validity in vehicle-terrain interaction simulation. Soil behavior being essentially nonlinear, various nonlinear relationships have been suggested by Kondner, Schofield-Wroth, Duncan-Chang and others to represent the nonlinear stress-strain behavior of soils. Recently, it has been shown (Ref. 1) that the parameters of nonlinear stress-strain relationships may be evaluated from field ring shear (Bevameter) tests, if properly conducted.

The scope of the present report is restricted to the analysis of deformations in frictionless clay soils. The Ramberg-Osgood relationship, first proposed some 40 years ago to model the strain hardening behavior of metals, was found to represent the nonlinear stress strain relationships of clay

soils, exhibiting strain hardening under rapid loading conditions, reasonably well. Since algorithms to treat material nonlinearities represented by the Ramberg-Osgood formula were already available in the finite element code, this formula has been accepted to represent the nonlinear stress strain behavior of the frictionless clay material assumed in the analyses.

The Ramberg-Osgood representation of nonlinear stress-strain properties is:

$$\varepsilon = \frac{\sigma}{E} + \frac{3\sigma_{0.7}}{7E} \left( \frac{\sigma}{\sigma_{0.7}} \right)^{n} \qquad (1)$$

where the three parameters defining the nonlinear relationship are:

$E$ = initial tangent modulus

$\sigma_{0.7}$ = stress at which the stress-strain curve has a secant modulus of $0.7E$

$n$ = exponent defining the rate of strain hardening in the plastic range.

Equation 1 is used in the finite element code to define the nonlinear stress-strain relationship in the plastic range, when the stress exceeds the yield point, $\sigma_0$ (Fig. 1). Up to that point, the stress-strain curve is linear. Strain upon unloading follows a linear path parallel to that in the elastic range, as shown in Fig. 1.

For the purposes of the analysis presented herein, the properties of the clay material were assumed to be represented by the following parameters:

$E$ = 800 psi

$\sigma_{0.7}$ = 4.3 psi

$n$ = 6.0

$\sigma_0$ = 5.0 psi

A clay material of medium plasticity and high degree of saturation exhibiting the properties defined by the above parameters would have a cone index in the range of 35 to 45.

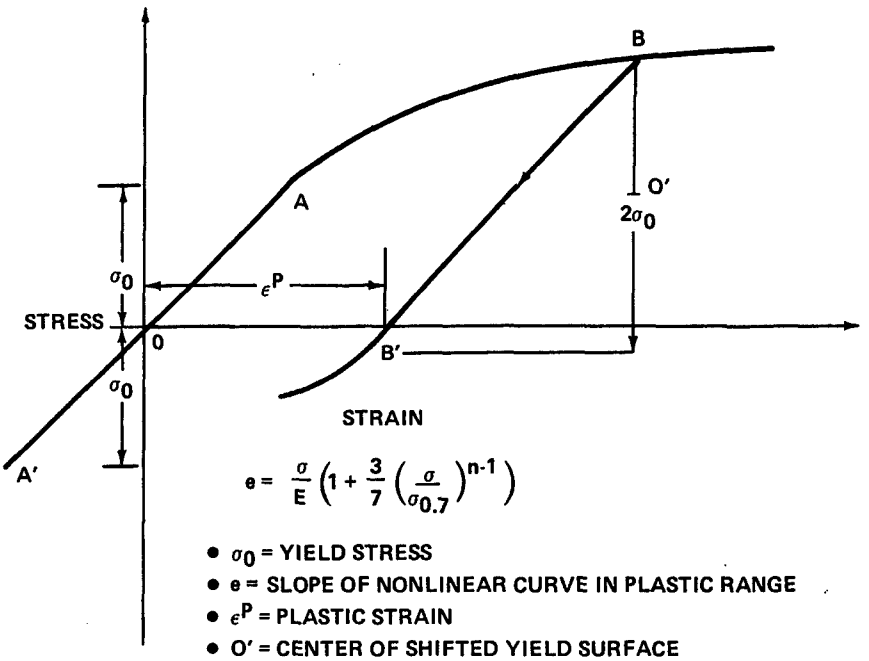


1874-001(T)

**Fig. 1 Ramberg-Osgood Representation of Nonlinear Strain Hardening Stress-Strain Relationship**

# 4. THE "DYCAST" FINITE ELEMENT CODE

The Dynamic Crash Analysis of Structures (DYCAST) code of the Grumman Research & Development Center was developed for the nonlinear, elastic-plastic, dynamic analysis of structures, primarily for the evaluation of the crashworthiness of various vehicle designs. For general information on the theoretical background of the code, the reader is referred to the DYCAST/GAC Theoretical Manual (Ref. 2). Program parameters and options, available elements, applicable nodal constraints and loading options are described in detail in the Users Manual (Ref. 3). The following discussion is limited to the adaptation of the code to the analysis of ground deformations beneath moving track loads, and problems associated with the use of the code for this purpose.

Of the elements available in the code, only the triangular membrane and the spring element were used in the analysis. Their usage is discussed in the next chapter. The triangular membrane element, defined by three nodes, used in the analysis assumes constant strain within the triangle. Transitional triangles are employed where different size triangles are joined in areas of mesh refinement. These triangles contain additional midside nodes, as necessary. To accommodate these additional nodes, a linear strain distribution is assumed within the transitional triangles.

Of the time integration method options available in the code the Explicit Modified Adams predictor-corrector method was used in the analysis presented herein. This integrator automatically chooses the time step to reflect current system stiffness and dynamic response.

Currently applied loading can be input in DYCAST in separable form,

$$P(x,t) = p(x)\, g(t)$$

where the $p(x)$ represents the spacial distribution of forces on node points and $g(t)$ is the time distribution of a load factor parameter. The function, $g(t)$ is input in DYCAST as a table of load factor versus time. Only one table is currently available in the code. Consequently, a new loading option has been added to the code to allow the simulation of the moving of the track load over the surface. This new option specifies a time delay between nodes

accepting concentrated loads. Combination of this option with the specification of loading time history under the key word "PTME" allows the simulation of traveling track loads, as shown in Fig. 2.

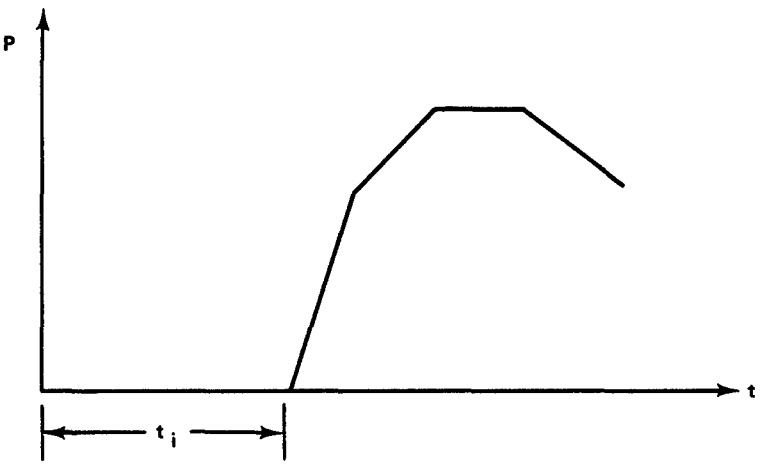


TIME RATE OF LOADING

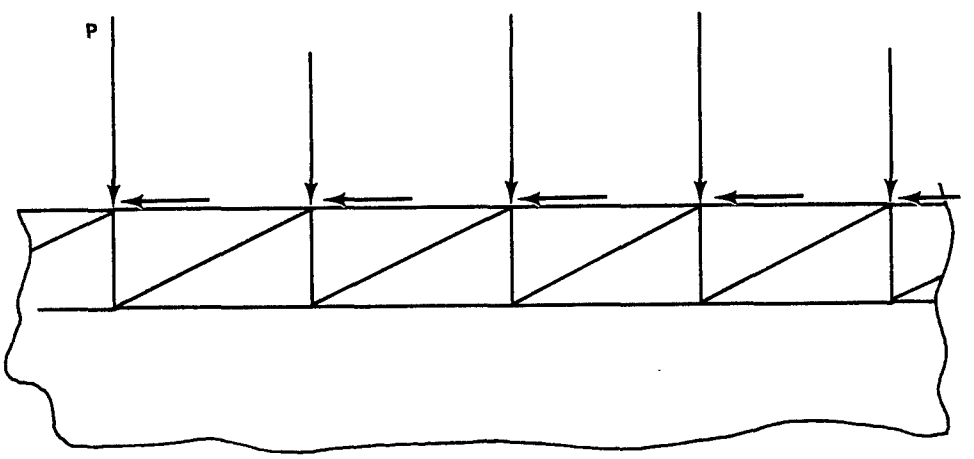


SPATIAL DISTRIBUTION OF LOADING

$t_i$ = TIME LAG SPECIFIED FOR EACH NODE

1874-002(T)

**Fig. 2 Time Delayed Loading Option**

## 5. DEVELOPMENT OF FINITE ELEMENT MESH

In vehicle-terrain interaction problems, the terrain is generally considered to be of large, often infinite extent. In the modeling of the behavior of such a continuum by a mesh of finite size, the conditions at the mesh boundaries require special attention. In dynamic analysis, rigid boundaries are the source of reflected stress waves which may or may not significantly affect the problem solution. In the present problem, the seat of soil deformations is in a shallow depth beneath the surface. The farther the mesh boundaries are from the seat of deformations the less the effect of the reflected stress waves on these deformations. Preliminary analyses were made to study the effect of stress waves on the deformations of the surface. The mesh used in the final analysis is shown in Fig. 3; nonlinear spring elements (not shown in Fig. 3) join the nodes at the vertical boundaries of the mesh. The parameters of these nonlinear spring elements were estimated on the basis of the magnitude of passive earth pressure and associated displacements at the node locations. These springs lessen the reflection of horizontal stress waves from these boundaries and simulate the restraining effect of the continuum adjoining the vertical boundaries of the mesh.

All nodes at the horizontal mesh boundary at 6 ft depth were assumed to be fixed for the following reasons. While stresses and displacements of the terrain are often computed by formulas valid for a semi-infinite half-space, in reality the soft soil conditions of particular interest in mobility research occur only to some limited depth where bedrock or other firm soil layer is encountered. Thus, in the vertical direction, it is more realistic to allow for a rigid boundary at some depth than to apply some artificial system there to simulate the effect of an adjoining infinite continuum of the same material.

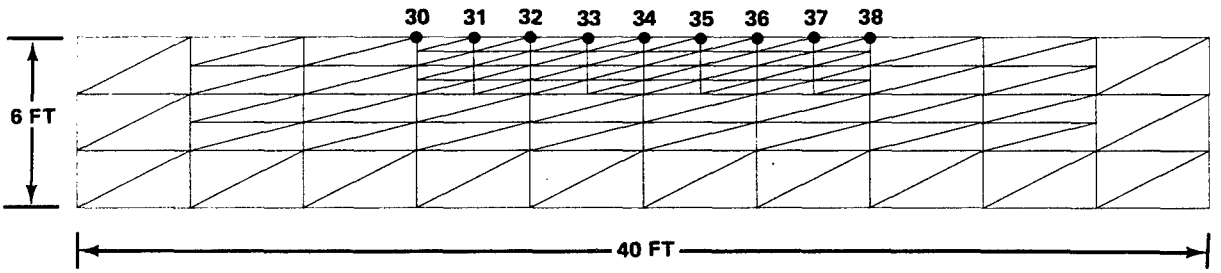


**Fig. 3 Finite-Element Mesh Developed for Analyses of Ground Deformations**

## 6. PRESSURE DISTRIBUTION PATTERNS

Tracked vehicles transmit vertical forces through road wheels and their suspension systems to the tracks. Tractive (horizontal) forces in the track are generated by the driving sprocket. The track pad and shoes distribute these forces over the contact area. Various patterns of pressure distribution result, depending on the relative stiffness of the suspension system and the ground, and the flexibility and initial tension of the track.

To evaluate the effect of pressure distribution on ground deformation, three pressure distribution patterns, have been selected for the analyses as shown in Fig. 4. All three are equivalent as far as total load is concerned and correspond to an average value of the vertical normal pressure of about 7.5 psi over the assumed 10 ft long x 1.25 ft wide contact area. For the convenience of reference, the pressure distribution at the top of Fig. 4 is called uniform, although allowance is made for a time rate of rise and decline of the uniform pressure over a 0.5 ft length at the ends of the contact area. The pressure distribution shown in the middle of Fig. 4 is referred to as a pattern with "low peaks," 1.58 times the uniform pressure. Between the peaks, there is a low pressure equaling 0.2 times the uniform pressure. The pressure distribution shown at the bottom of Fig. 4 is a pattern with "high peaks", 2.12 times the uniform pressure. The areas between the peaks carry no load.

The horizontal or tangential stress as transmitted to the ground are assumed to be distributed in the same pattern as the vertical normal stresses. Their magnitude is assumed to be in a selected proportion to the vertical stresses. Several horizontal/vertical stress ratios have been selected in the analysis to evaluate the effect of this ratio on ground deformations.

The assumed pressure distributions are idealizations of distributions observed in various field experiments and represent a realistic approximation of pressure distribution variations expected to occur beneath tracks supported by five road wheels.

Since the triangular elements of the finite element code accept only loads concentrated at the nodes, the pressure distribution patterns were converted to concentrated loads acting on nodes 30 - 38 (Fig. 3).

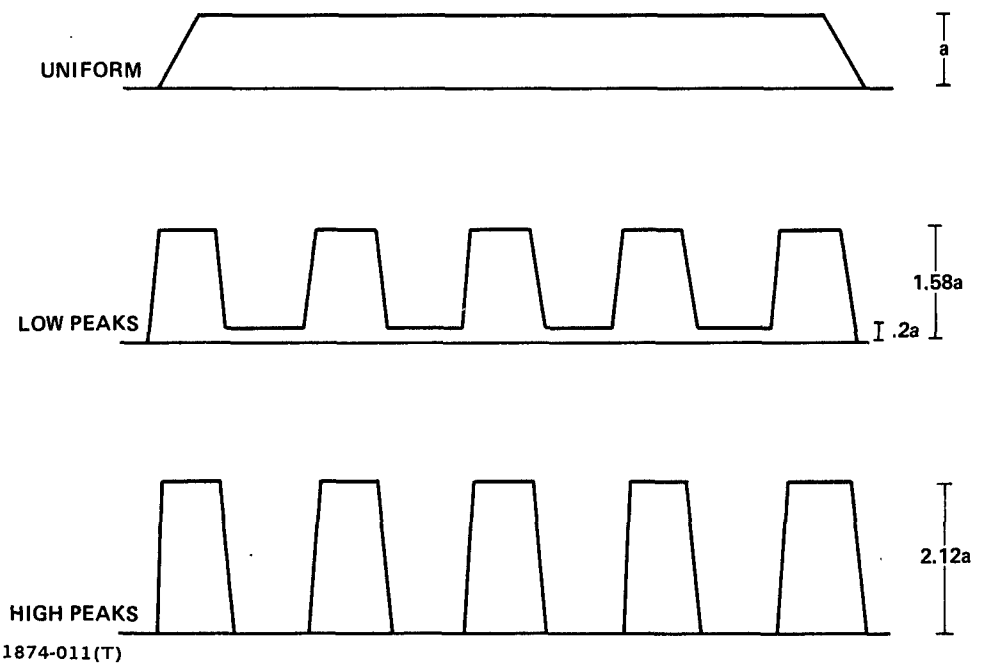


**Fig. 4 Patterns of Pressure Distribution Assumed in the Analyses**

## 7. SIMULATION OF VEHICLE TRAVEL

The representation of a continuum of large horizontal extent with a relatively small finite mesh, poses problems for the simulation of traveling vehicle loads. The following two alternatives were considered for the simulation.

- The vehicle is assumed to travel at steady speed
- The vehicle accelerates from a standing position to a given speed and maintains that speed during passage of the vehicle over a point in the ground.

While this latter assumption is the desirable choice, its adoption would have required a much larger mesh than that shown in Fig. 3 and appreciable computer time for the analysis, since computations for the accelerating state increase the total time significantly. The assumption of steady state speed, on the other hand, involves approximations in regard to the loads applied at the surface.

The assumption of steady state speed implies that the vehicle arrives at the mesh boundary with that steady speed. Thus, all nodes at the surface should receive loads for a duration appropriate for the travel velocity. However, the triangular elements adjoining the vertical boundary of the mesh are, except for the nonlinear springs, laterally unsupported and would, therefore, exhibit excessive and unrealistic strains if directly loaded. The compromise solution, adopted in the analysis, is that loading for a vehicle traveling from left to right starts at Node 30 and continues through Node 38 (Fig. 3). The track position of interest is when the loading reaches Node 38. At this time, the 10 ft contact length of the track covers five triangular blocks ending at Node 33. A typical deformed mesh corresponding to this position of the track is shown in Fig. 5. Ground deformations in this position are thought to be representative of those occurring beneath a vehicle traveling at steady speed, hypothetically from an infinite distance. The deformations to the left of Node 33 are not necessarily representative of those occurring behind a tracked vehicle traveling at steady speed and definitely do not signify a rebound but rather the lack of loading in this part of the surface.

The role of the part of the mesh to the left of the Node 33 is to simulate the action of the continuum behind the track, and not the determination of the deformations of that region.

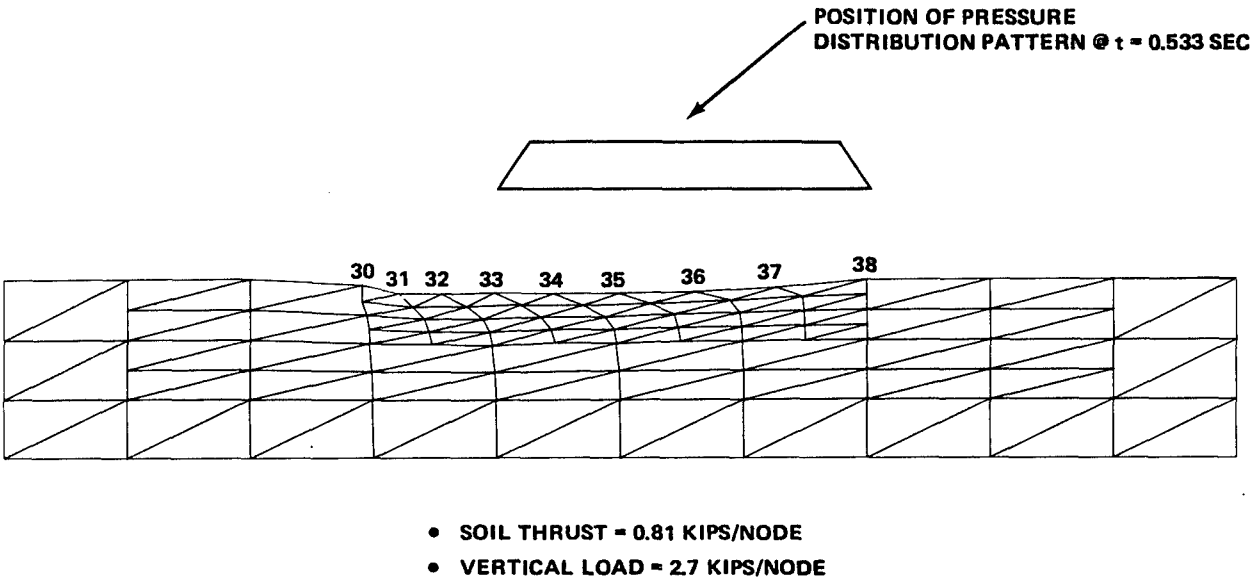


1874-004(T)

Fig. 5 Mesh at t = 0.533 sec Time, Deformed Under Uniform Pressure Moving at 30 ft/sec

## 8. CASES ANALYZED

In accordance with the scope of this project, the effect of the following input variations on ground deformation has been investigated:

- Soil thrust (tractive force)
- Pressure distribution
- Speed.

To keep the total number of analyses to a reasonable level, the effect of each of these input variables was analyzed for one combination of the other input variables only. The matrix of the analyzed cases is shown below.

| SPEED, FT/SEC | $F_h/F_v$ | | | | | | | | |
|---|---|---|---|---|---|---|---|---|---|
| | BRAKING | | | DRIVING | | | | | |
| | -.5 | -.3 | -.1 | 0 | .1 | .3 | .5 | .67 |
| 10 | | | | | | U | | |
| 15 | | | | | | H,U,L | | |
| 20 | | | | | | L | | |
| 30 | U | U | U | U | U | H,U,L | U | U |
| 60 | | | | | | H,U,L | | U |

$F_h$ = Horizontal force (soil thrust)

$F_v$ = Vertical force

U = Uniform pressure distribution

L = Pressure distribution with "Low peaks"

H = Pressure distribution with "High peaks"

## 9. RESULTS OF THE ANALYSIS

The analysis of ground deformations beneath moving track loads brought forth an abundance of information on the time history of stresses in each element and displacements of each node of the mesh representing the soil mass. For brevity, only those results are reported herein which have direct bearing on track performance.

Figure 6 shows the variation of soil thrust with slip due to ground deformation for the case of uniform pressure distribution. Soil thrust is the propelling force from which the motion resistance would have to be deducted to obtain the net drawbar pull. The major component of the motion resistance is due to the trim angle, obtained in the analyses. The dotted line in Fig. 6 shows the soil thrust minus motion resistance due to trim angle values approximating the drawbar pull. Point "A" in the figure indicates the case for which the deformed mesh is shown in Fig. 5.

The slip value shown in Fig. 6 is an average value of that portion of the slip which is caused by ground deformation. Note that ground deformation itself may be responsible for as high a slip as 20%.

Other components of the total slip include the slip due to tire deformations and separation of the solid-soil interfaces. The magnitude of the former is difficult to estimate but in all probability it is much smaller than that caused by ground deformation.

Separation of the solid-soil interfaces may occur whenever the shear stress exceeds the strength of the interface. This will be discussed in more detail later in connection with the displacement and velocity history of the individual nodes during passage of the track load.

Figure 7 shows the variation of sinkage with soil thrust for uniform pressure distribution for the whole range of soil thrust. The effect of pressure distribution with low and high peaks is shown for a limited range of soil thrust, encountered most commonly in driving conditions. At the right side of the figure, the coefficient of motion resistance due to the trimmed position of the track is shown. The solid line indicates that even pressure distribution is most helpful in keeping sinkage and motion resistance low; the

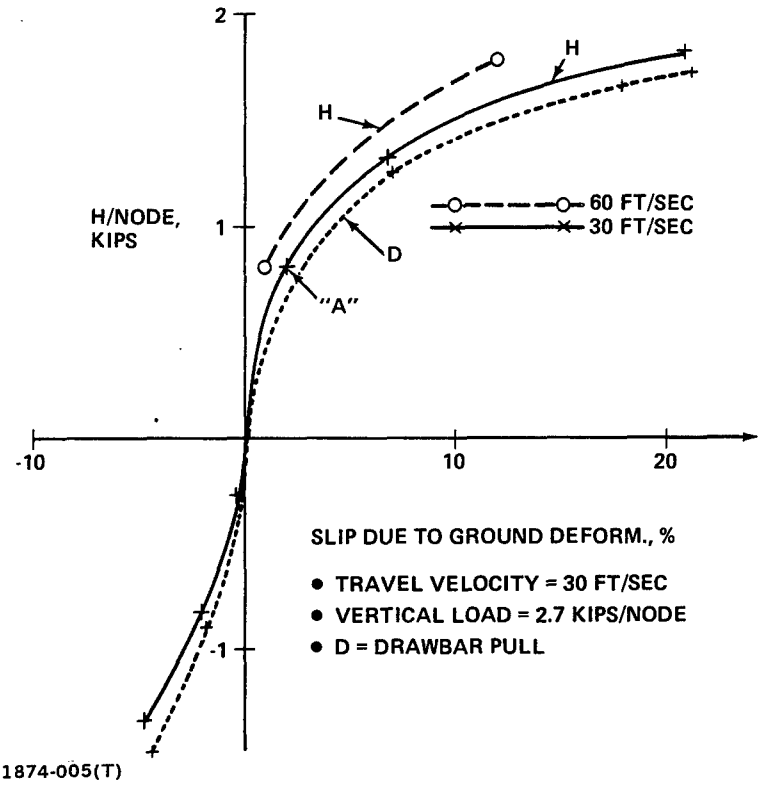


**Fig. 6 Soil Thrust (H)-Slip Relationship for Uniform Pressure Distribution**

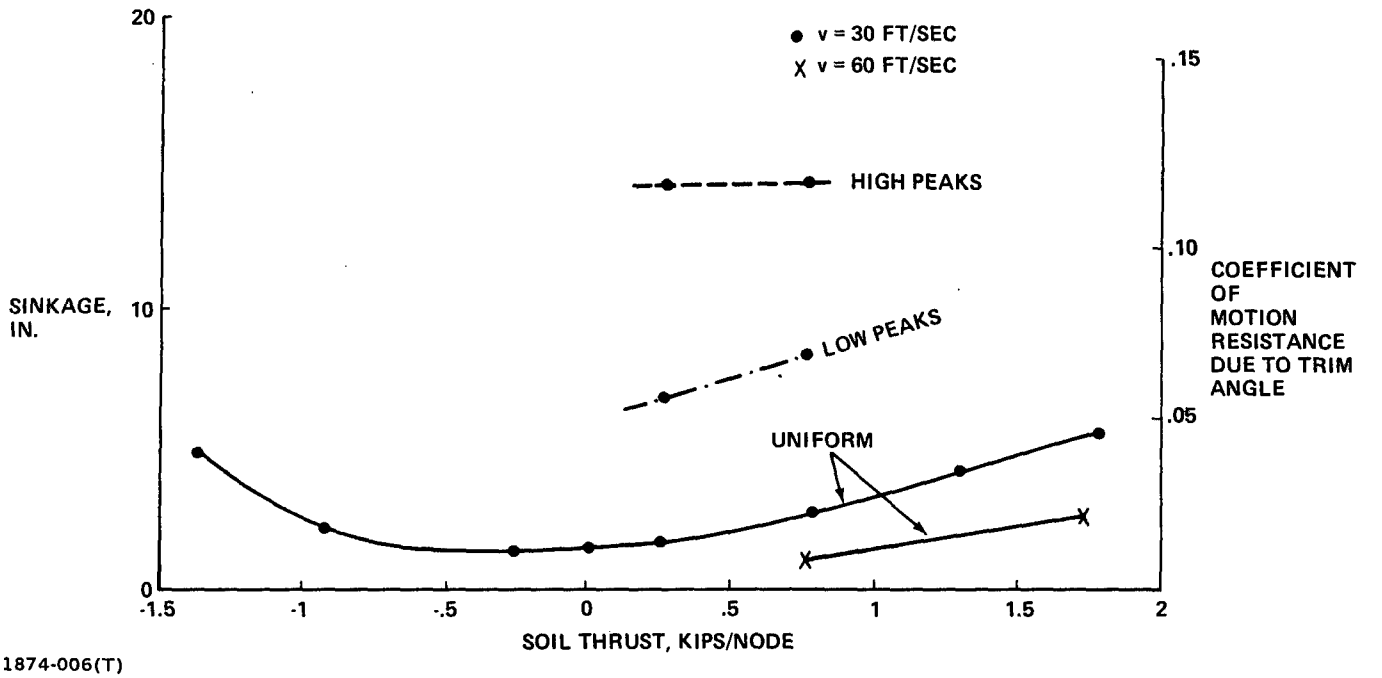


**Fig. 7 Effect of Soil Thrust & Pressure Distribution Pattern on Sinkage & Coefficient of Motion Resistance**

increase of sinkage with the absolute value of soil thrust is the most important feature of track-soil interaction.

Figure 8 shows the effect of speed and pressure distribution on sinkage and the motion resistance generated by the trimmed position of the track. It is apparent from the figure that, from the motion resistance point of view, evenly distributed pressures and high travel velocity are the most advantageous. An increase in the travel velocity from 10 to 60 ft/sec reduces the sinkage to about half of its maximum value exhibited at 10 ft/sec in the case of uniform pressure distribution and even more in the case of pressure distributions with peaks. For the case indicated by "B" in the figure, the deformed mesh is shown in Fig. 9.

The magnitude of slip caused by the horizontal deformation of the ground is also affected by both the pressure distribution and travel velocity. Figure 10 shows the variation of slip with the pressure distribution pattern and travel velocity for a soil thrust of 0.81 kips/node, 30% of the vertical load/node. This useful and novel information on the interrelationship among slip, pressure distribution and track velocity refers to one type of clay soil. More important than the results shown in the figure for this soil is that the methodology to obtain such information has been developed and can be applied to other cases.

Displacements, velocities and accelerations of each node are computed for every time increment by the integration of the differential equations of motion. Of these, the displacements and velocities of the loaded nodes at the surface are of particular interest, since the vertical displacements of the surface nodes may be equated with sinkage and the horizontal displacements are the principal cause of slip. An example of the time history of x (horizontal) and y (vertical) displacements is shown in Fig. 11 for Node 33 for the case of a pressure distribution with low peaks and 30 ft/sec travel velocity. The effect of pressure variation is barely discernible in the plots. The total horizontal displacement of this node at the time it was just passed by the moving track load ($t = 0.5333$ sec) is opposite to the direction of travel and, in effect, reduces the distance traveled. This travel reduction is identified as slip in off-road mobility research terminology.

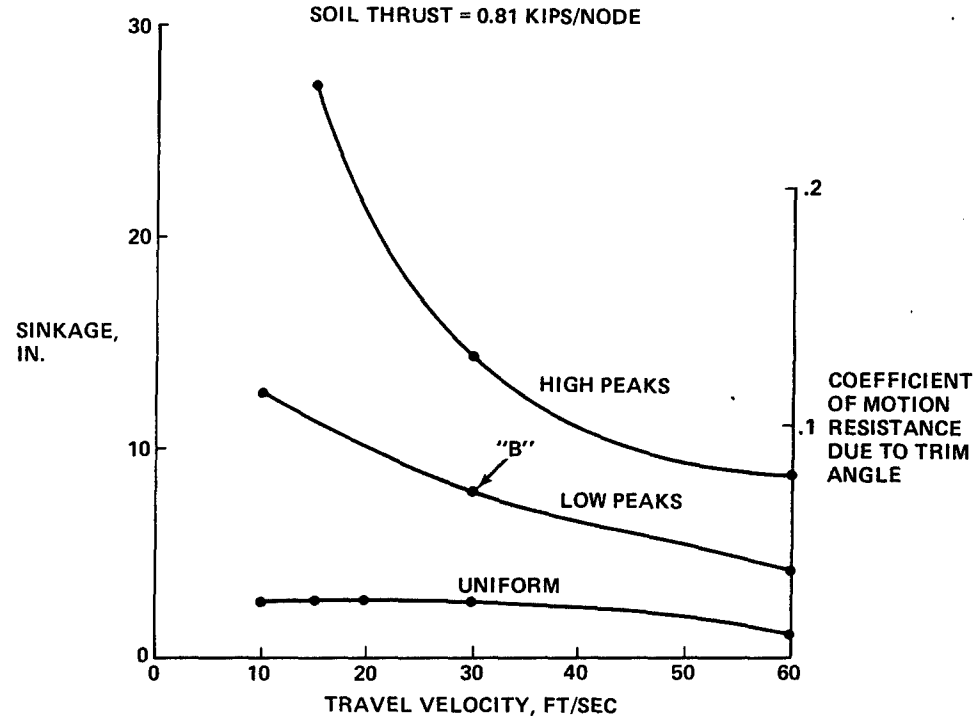


**Fig. 8 Effect of Travel Velocity & Pressure Distribution Pattern on Sinkage & Coefficient of Motion Resistance**

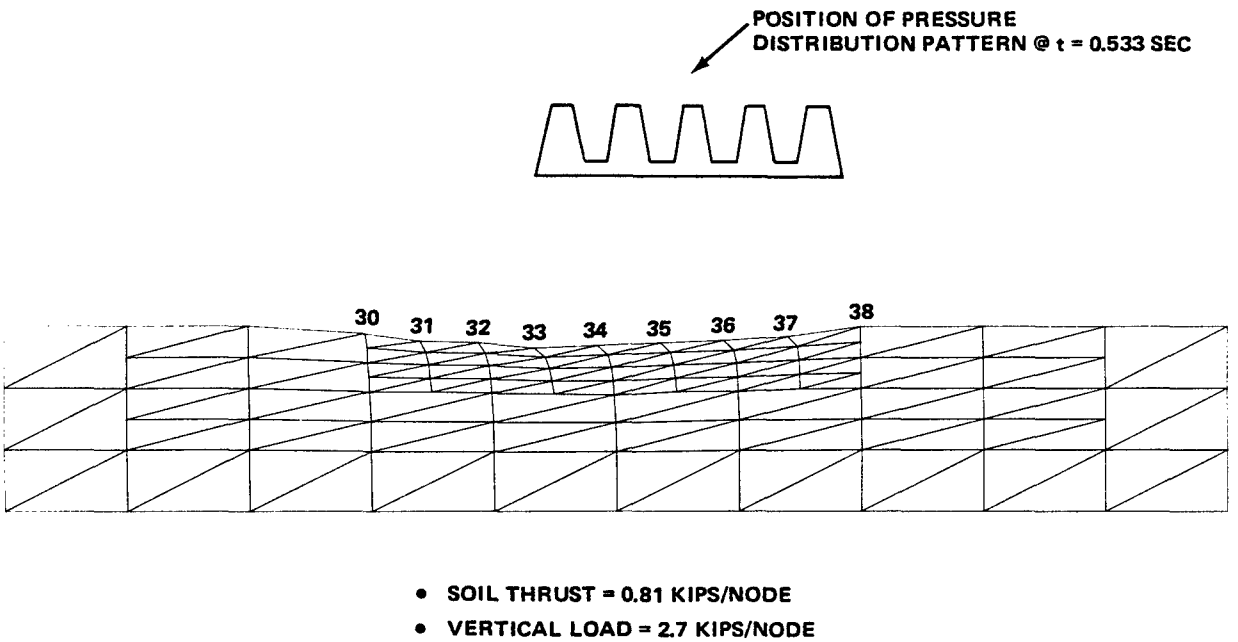


Fig. 9 Mesh at t = 0.533 sec Time, Deformed Under Pressure Distribution Pattern with Low Peaks, Moving at 30 ft/sec

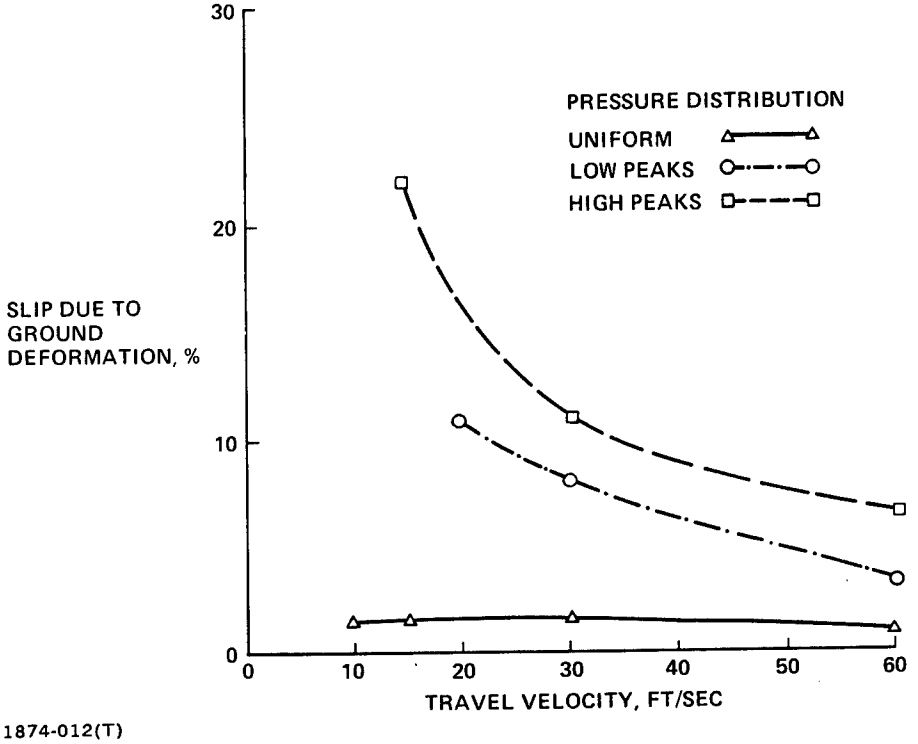


1874-012(T)

**Fig. 10 Effect of Travel Velocity & Pressure Distribution Pattern on Slip Associated with the Development of Soil Thrust Amounting to 30% of Vertical Load**

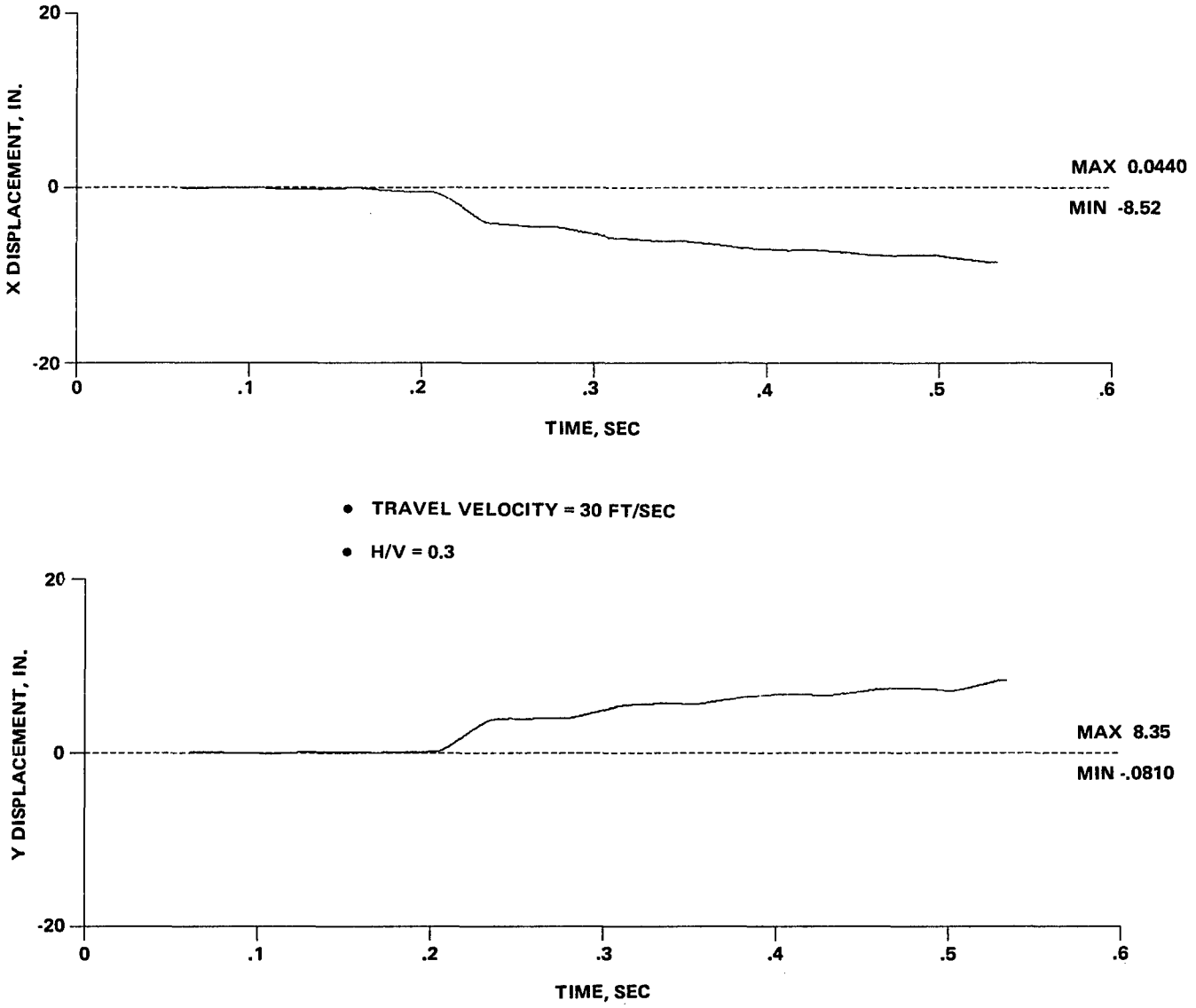


1874-009(T)

Fig. 11 Time Histories of X and Y Displacements of Node 33, Pressure Distribution with Low Peaks

The time histories of x and y velocities of the same node, shown in Fig. 12, reveal that the slip is not uniform over the length of the contact area. The velocity variations reflect the changes in the pressure distribution. From the travel velocity and average slip, the track velocity computes as 32.8 ft/sec on the average. The first peak in the x velocity occurs shortly after the loading of Node 33 begins at t = 0.2 sec. The amplitude of the peak far exceeds the average track velocity indicating that the assumed rate of loading is too high. To eliminate this inconsistency, the development of an interface element, simulating the load transfer between track and soil, is recommended. Such an element would allow for relative displacements between track and soil and the development of shear stresses consistent with an interface shear strength-displacement relationship.

The y velocities shown in Fig. 12 also show the response of the soil to the pressure impulses represented by the peaks in the pressure distributions. It is interesting to note that between the positive (downward) velocity peaks the velocities become negative (upward) corresponding to a soil response that tends to flex the tracks upward in between the road wheels.

The pressure distribution pattern and travel velocity define the rate of increase (and decrease) of the load transmitted to the soil. For the example shown in Fig. 11 and 12, this rate is comparable to that experienced with tanks upon gun firing. The finite element method, preferably with the previously mentioned interface element added, is essentially a (and probably only) suitable method for the study and evaluation of the soil response to such impulsive loadings.

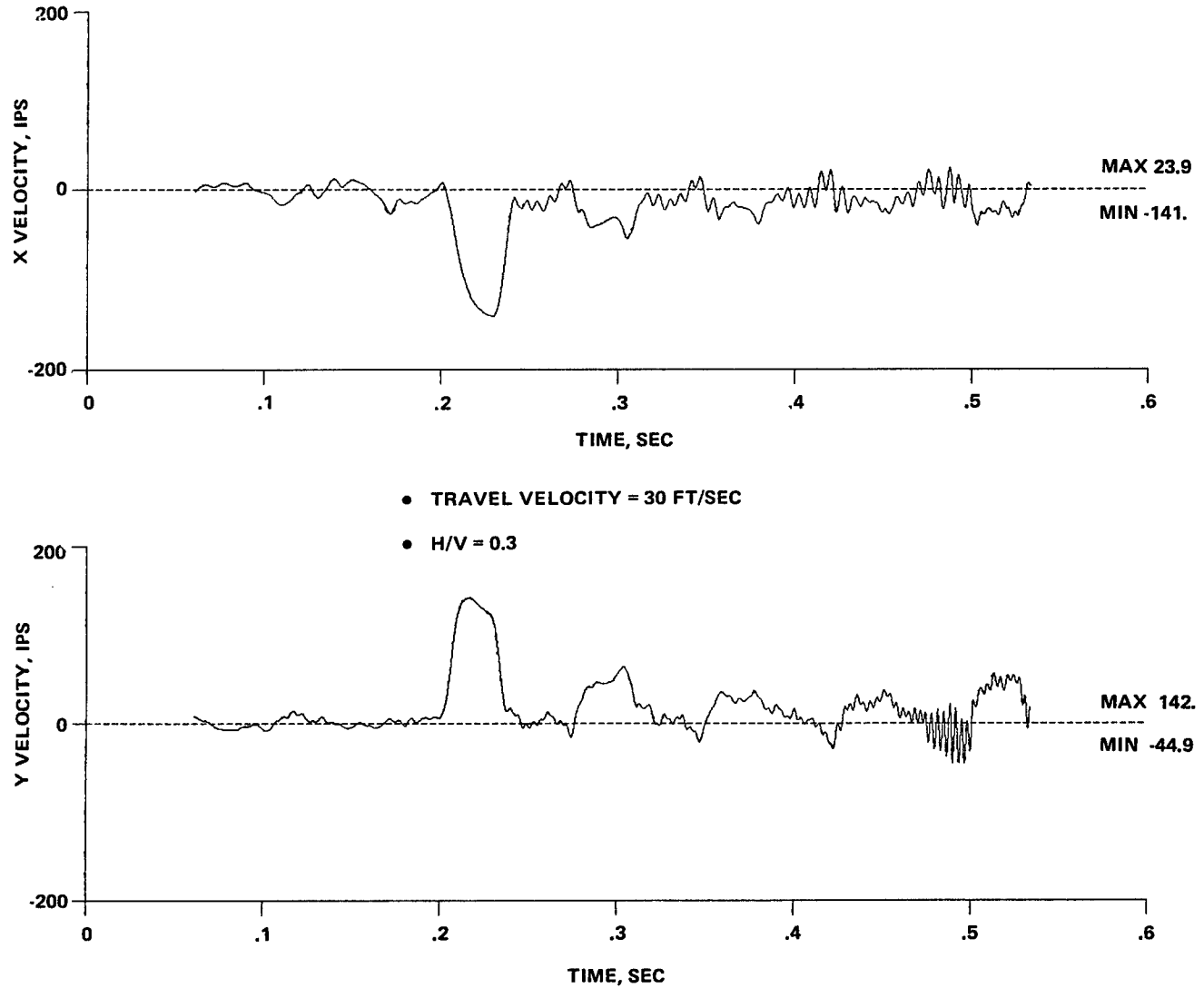


Fig. 12 Time Histories of X and Y Velocities of Node 33

# 10. CONCLUSIONS & RECOMMENDATIONS

A methodology, using finite element analysis techniques, has been developed for the determination of the deformation of clay soils under moving track loads. Nonlinear stress-strain properties as well as plastic behavior of soil have been modeled and together with the dynamic capabilities of the finite element code fully utilized in the analyses. This methodology, for the first time in off-road mobility research, makes the quantitative evaluation of the effect of pressure distribution and travel velocity on soil deformation induced slip, trim angle and motion resistance feasible. Results of the analysis of selected cases, shown graphically, indicate that these effects are significant. The method is also suitable for the performance of parametric analysis needed for design optimization.

It is recommended that the method be expanded to include an appropriate model of frictional soil behavior.

The method is also suitable for the analysis of soil response to impulsive loadings. The rate of rise of loading for the assumed travel velocities and peaks in the pressure distribution is of the same order of magnitude as experienced with the rise of road wheel loads upon gun firing. However, for the analysis of soil response to impulsive load, the development of an interface element that would allow for the relative displacement of track and soil, is recommended.

## 11. REFERENCES


1. Janosi, Z.J. and Karafiath, L.L., "Improved Technique of Field Ring Shear Testing for Soil Strength Determination," Proc 7th Int Conf for Terrain Vehicle Systems, Calgary, Canada, Aug 1981

2. "DYCAST/GAC Nonlinear Structural Dynamic Finite Element Computer Code Theoretical Manual," Grumman Aerospace Corporation R&D Center Report RE-501, Aug 1974

3. "DYCAST/GAC Nonlinear Structural Dynamic Finite Element Computer Code Users Manual, Version 1.1," Grumman Aerospace Corporation R&D Center, June 1982

DISTRIBUTION LIST
(As of 1 January 1983)

Please notify USATACOM, DRSTA-ZSA, Warren, Michigan 48090, of corrections and/or changes in address.

Superintendent
US Military Academy
ATTN: Dept. of Engineering
Course Director for
Autmv Engineering
West Point, NY 10996. . . . . (01)

Commander
US Army Logistic Center
ATTN: ATCL-CC
Mr. J. McClure
Ft. Lee, VA 23801 . . . . . (01)

US Army Research Office
P.O. Box 12211
ATTN: Dr. David Mann
Research Triangle Park, NC 27709 (01)

HQDA
Office of Dep Chief of Staff for Rsch
Dev & Acquisition
ATTN: Dir of Army Research, ARZ-A
Dr. Lasser
Washington DC 20310 . . . . . (01)

Commander
US Army Mobility Equipment
R&D Command
ATTN: DRDME-RT
Ft. Belvoir, VA 22060 . . . . . (01)

Director
US Army Corps of Engineers
Waterways Experiment Station
P.O. Box 631
ATTN: Mr. Nuttall
Vicksburg, MS 39180 . . . . . (01)

Director
US Army Cold Regions Research
& Engineering Lab
P.O. Box 282
ATTN: Dr. Liston
Library
Hanover, NH 03755 . . . . . (01)

Commander
US Army Test & Evaluation Command
Aberdeen Proving Grounds
ATTN: AMSTE-BB
AMSTE-TA
APG, MD 21005 . . . . . (02)

Commander
Rock Island Arsenal
ATTN: SARRI-LR
Rock Island, IL 61201 . . . . (02)

Commander
US Army Yuma Proving Ground
ATTN: STEYP-RPT
STEYP-TE
Yuma, AZ 85364 . . . . . (02)

Director
US Army Human Engineering Lab
Aberdeen Proving Grounds
ATTN: Mr. Eckles
APG, MD 21005 . . . . . (01)

Director
US Army Ballistic Research Lab
Aberdeen Proving Grounds
APG, MD 21005 . . . . . (01)

Director
US Army Material Systems Analysis
Agency
Aberdeen Proving Grounds
ATTN: Mr. Harold Burke
APG, MD 21005 . . . . . (01)

Director
Defense Documentation Center
Cameron Station
Alexandria, VA 22314 . . . . (12)

Director
National Tillage Machinery Lab
Box 792
Auburn, AL 36830 . . . . . (01)

Director
USDA Forest Service Equipment
Development Center
444 East Bonita Avenue
San Dimes, CA 91773 . . . . (01)

Director
Keweenaw Research Center
Michigan Technological Univ
Houghton, MI 49931 . . . . (01)

Engineering Society Library
345 East 47th Street
New York, NY 10017 . . . . (01)

Dr. M. C. Bekker
224 East Islav Drive
Santa Barbara, CA 93101 . . (01)

Mr. R. S. Wismer
Deere & Company
Engineering Research
3300 River Drive
Moline, IL 61265 . . . . (01)

The University of Iowa
ATTN: Dr. E. Haug
Iowa City, IA 52242 . . . . (01)

Stevents Institute of Technology
Castle Point Station
ATTN: Irmin Kamm
Hoboken, NJ 07030 . . . . (02)

SFM
Forsvaretsforskningsanstalt
Avd2
Stockholm 80, Sweden . . . . (01)

Mr. Hedwig
RU III/6
Ministry of Defense
5300 Bonn, Germany . . . . (02)